www.ptcer.pl/mccm

MATERIAŁY CERAMICZNE /CERAMIC MATERIALS/, 62, 4, (2010), 490-495

Protective Coating to Suppress Degradation of $CoSb_3$ Thermoelectric at Elevated Temperatures

E. Godlewska, K. Zawadzka*, R. Gajerski, M. Mitoraj, K. Mars

AGH University of Science and Technology, Faculty of Materials Science and Ceramics, Al. Mickiewicza 30, 30-059 Krakow, Poland
*e-mail: zawadzka.kinga@gmail.com

Abstract

A polymer-metal hybrid coating has been developed to prevent degradation of the $CoSb_3$ skutterudite in contact with air at elevated temperature. Uncoated and coated $CoSb_3$ specimens were exposed to air at 500, 600 and 700°C for up to 80 hours. The performance of materials was evaluated on the basis of mass changes, visual inspection, and systematic analysis of specimen surfaces, fractures and cross-sections in terms of the chemical and phase composition as well as microstructure. It has been found that the coating system used in this work was effective up to 600°C. It significantly reduced the access of gases, extent of oxidation and sublimation of antimony which limit the lifetime and efficiency of thermoelectric generators.
Keywords: Coating, Microstructure, Methylphenylsiloxane paint, Thermoelectric generator, $CoSb_3$

POWŁOKA OCHRONNA TŁUMIĄCA DEGRADACJĘ TERMOELEKTRYKU $CoSb_3$ W PODWYŻSZONYCH TEMPERATURACH

Opracowano hybrydową powłokę polimerowo-metalową do ochrony przed degradacją w powietrzu w podwyższonej temperaturze skutterydu $CoSb_3$. Pokryte powłoką i nie pokryte próbki $CoSb_3$ wystawiono na działanie powietrza w temperaturach 500, 600 i 700°C przez okres trwający do 80 h. Osiągniętą jakość materiałów oceniono na podstawie zmian masy, sprawdzenia wzrokowego i systematycznej analizy powierzchni próbki, przełomów i przekrojów w kategoriach składu chemicznego i fazowego, a także mikrostruktury. Stwierdzono, że system powłoki wykorzystany w pracy był efektywny do 600°C. Redukuje on znacznie dostęp gazów, zasięg utlenienia i sublimacji antymonu, ograniczających czas pracy i wydajność generatorów termoelektrycznych.
Słowa kluczowe: powłoka, mikrostruktura, farba metylo-fenylo-siloksanowa, generator termoelektryczny, $CoSb_3$

1. Introduction

Skutterudites belong to the most promising materials for the application in thermoelectric generators. At temperatures exceeding the range 400–700°C, the figure of merit *ZT* of doped $CoSb_3$ can be bigger than 1 [1]. Unfortunately, at these temperatures $CoSb_3$ is not stable. It has been observed that oxidation of $CoSb_3$ starts even at 380°C [2, 3]. Another significant problem with using cobalt antimonide at elevated temperatures is constitued by the antimony loss by evaporation or oxidation.

Hara *et al*. [4] investigated oxidation of undoped $CoSb_3$ at 600°C in air and found two oxide layers on the surface of specimens. The outer one contained three phases of antimony oxides: β-Sb_2O_4, Sb_2O_4 and Sb_2O_3. The subjacent layer contained four phases: Sb_2O_4 and β-Sb_2O_4, and two cobalt-antimony oxides, $CoSb_2O_6$ and $CoSb_2O_4$. The outer layer was much thinner than the inner one, 16 μm and 32 μm, respectively. Other studies on the behaviour of CoSb3 powders in air at temperatures ranging from 20 to 850˚C also indicated the formation of $CoSb_2O_6$, $CoSb_2O_4$ and Sb_2O_4 [5].

The oxide layers on the specimen surface can play a role of barrier slowing down, to some extent, the outward diffusion of antimony when oxidation is continued. However, the protection provided by those oxide layers is by far not sufficient. There is a strong need of developing an efficient coating to prevent compositional changes of $CoSb_3$ at elevated temperatures. Some coating systems for *n*-type $CoSb_3$ and *p*-type $CeFe_3RuSb_{11}$ are under development in Jet Propulsion Laboratory [6]. As oxygen is not present in the space environment, the most important problem in this application is to prevent the antimony loss by sublimation. The investigations carried out so far have been focused on metallic coatings, such as Nb [7], nevertheless interesting results have been reported with ceramic coatings, *e.g.* $MgAl_2O_4$ [8], which prevented antimony sublimation at 700°C.

For the terrestrial applications of $CoSb_3$, it is necessary to develop a coating system, which would not only prevent antimony loss by sublimation but also by oxidation. Moreover, it should withstand thermal cycling at elevated temperatures and should not adversely affect thermoelectric proprieties of the substrate. The objective of this work was to assess the usefulness of methylphenylsiloxane paints with lamellar Al filler or spherical Cr filler as protective coatings for $CoSb_3$.

2. Experimental

The $CoSb_3$ specimens were prepared from elemental powders mixed in an adequate stoichiometric ratio. The synthesis was conducted in the evacuated quartz ampoules at 700°C for 168 h. The obtained powder product was consolidated by hot-pressing and then cut with a diamond saw into pellets, diameter of 10 mm and thickness of 1-2 mm. The phase composition of the powder product was confirmed by X-ray diffraction (XRD). Density of the sintered specimens, measured by a hydrostatic method, was > 98 % theoretical density.

The coating was applied by an immersion method. A mixture of siloxane resins dissolved in xylene was used as a binder and powder of Al or Cr as a filler. To improve coating adherence, the surface of specimens was sand-blasted (electrocorundum, grain size of 340 μm). After deposition and drying, the coating was cured at 250°C for 2 h.

For the preliminary experiments with Al coating, one side of the pellets was covered with a single layer and the other side with a double layer. As the single-layer coating was not protective enough, next experiments were performed with double-layer coatings. Fig. 1 shows the specimen surface with as-received coatings. Brighter spots represent Al or Cr filler particles embedded in a siloxane resin. In the case of Al-polymer coatings, they were bigger in size. (Figs. 1a and 1b).

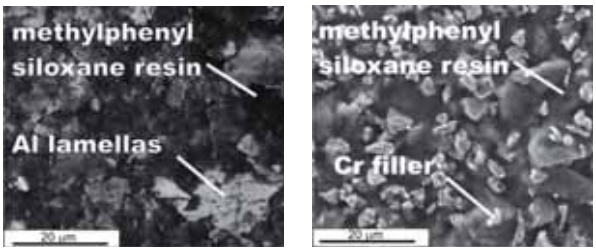

a) b)

Fig. 1. SEM images of coated samples surface a) with Al filler, b) with Cr filler.

The coated specimens were oxidised under thermal-cycling conditions. Before the tests, they were weighed and measured. Oxidation of reference specimens was conducted in the same conditions. Four cycles, each of 20 h dwell time, were performed. In each test a set of three specimens was used, the specimens being positioned vertically in separate ceramic crucibles. This enabled an easy access of oxygen to specimen surface and collection of any oxide or coating spallations. The crucibles were placed in a ceramic boat and inserted into the hot furnace. After each cycle of 20 h at temperature, the specimens were gradually air-cooled during 15 minutes and then weighed. Because of very fast degradation of the unprotected material at 700°C only three 20-hour cycles were performed. After each cycle one of the three specimens was removed for analysis.

In the case of coated specimens, the oxidation process was conducted similarly as without coating at 500°C and 600°C, except that in first cycle specimens were heated with the furnace at a rate of 5°C/min.

The experiments at 700°C revealed that the double-layer Al-polymer coating was not resistant to thermal cycling. Spallation was observed after each cooling step.

In the case of polymer-chromium coating, complete spallation occurred for one pellet only at 700°C and that pellet was removed for analysis already after one cycle. For other specimens, the test was continued up to 80 h. Small amounts of spalled material were collected in alumina crucibles but the coating itself was adherent.

The post-test examination of the specimens comprised scanning electron microscopy (SEM) and X-ray diffraction (XRD). Cross-sections of specimens were examined by SEM using secondary electron images and energy dispersive X-ray spectroscopy (EDS).

3. Results and discussion

3.1. $CoSb_3$ without coating

It can be seen in Fig. 2 that the mass of specimens increased with oxidation time, indicating formation of a solid oxidation product. The question about volatile species produced simultaneously remains open, since those were not analysed. It can be seen clearly that the mass of specimens increased quicker during the second cycle of oxidation. Evaporation of some volatile species might occur during the first cycle. Then this process was probably suppressed by a layer of antimony oxides formed on the specimen surface during the first 20 h. This behaviour is consistent with the results published by Hara *et al.* [4], who stated that thickness of the first antimony oxide layer was proportional to the square root of oxidation time, thus indicating diffusion control. The growth rate of the scale on specimens oxidised at 600°C was much faster than at 500°C. The same tendency was observed when comparing the kinetics of scale growth at 600°C and 700°C. The average percent mass change of specimens during the consecutive 20-h cycles is given in Table 1. The quickest oxygen uptake occurs during the second cycle.

With the increasing temperature the scale structure becomes thicker and more complex, as shown in Figs. 3a-f. After 80 hours the scale on the $CoSb_3$ specimen, oxidised at 500°C, was about 5 μm thick. According to the EDS analyses the dominant components were Sb and O and the minor one was Co (about 2 at.%), indicating the presence of antimony oxides. According to EDS analyses of the specimens oxidised for 80 hours at 600°C, cobalt was not present in the outermost layer. However, the subjacent layer contained substantial amounts of this element (about 12 at.% and atomic ratio Co:Sb = 1:2). This suggested formation of binary cobalt-

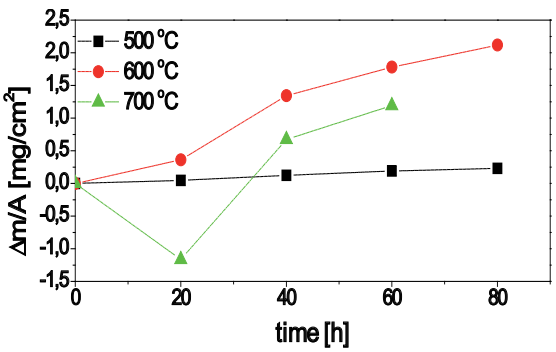

Fig. 2. Mass changes of uncoated $CoSb_3$ specimens during cyclic oxidation in air.

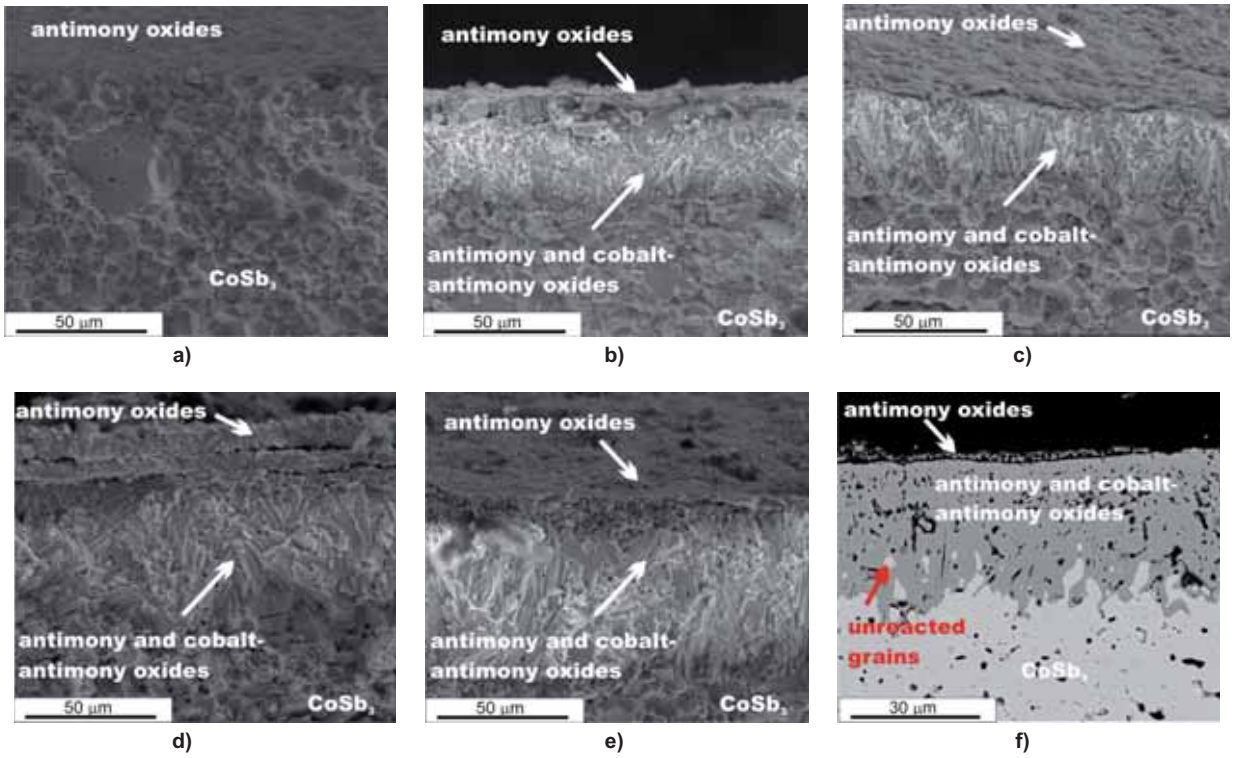

Fig. 3. SEM images of fractures of uncoated $CoSb_3$ specimens after exposure: a) 500°C/80h, b) 600°C/80h, c) 700°C/20h, d) 700°C/40h, e) 700°C/60h, and f) cross-section after exposure 700°C/60h.

antimony oxides. The second layer was much thicker than the first one, *i.e.* 30 μm and 10 μm, respectively. The scale on the specimen oxidised for 20 h at 700°C, consisted of two layers. The inner was about 30 μm and the outer a few micrometers thick. After 40 h, three layers could be distinguished near the surface. The outermost was 10 μm thick and contained Sb and O. The layer located beneath contained 10 at.% Co, and was about 10 μm thick. The third, innermost layer was composed of Sb, O and 12 at.% Co and was ≤ 50 μm thick. The analyses after a 60-h exposure at 700°C gave results comparable to the above described but the innermost layer was more than 50 μm thick.

As it can be seen in Fig. 3f, the scale/substrate interface was corrugated and some unreacted $CoSb_3$ grains were still present in the innermost scale layer. It seems that degradation of the material proceeded along the grain boundaries. SEM images from the inner regions of specimens revealed porosity and internal oxides located in the grain boundaries, which might adversely affect mechanical properties. Specimens prepared for microscopic observations were heavily cracked, probably while being pressure-mounted in a resin (Fig. 4).

The phase composition of the scale was determined by XRD. For the specimens oxidised at 500°C, the scale components were: Sb_2O_4, β-Sb_2O_4 and Sb, while at 600°C - Sb_2O_4, β-Sb_3O_4, Sb_2O_3, $CoSb_2O_6$, $CoSb_2O_4$ and Sb_2O_2. Phases identified after oxidation at 700°C were the following: $CoSb_2O_6$, $CoSb_2O_4$, $CoSb_2$ and Sb_2O_4. Based on the complex XRD, SEM and EDS analyses, it can be stated that the large needle-like crystals in the innermost scale layer, oriented perpendicularly to the specimen surface, were built of cobalt-antimony oxides. The outgrowing crystals on the scale surface were built of antimony oxides.

The EDS concentration profiles of elements across the scale/substrate interface showed a stepwise decrease of

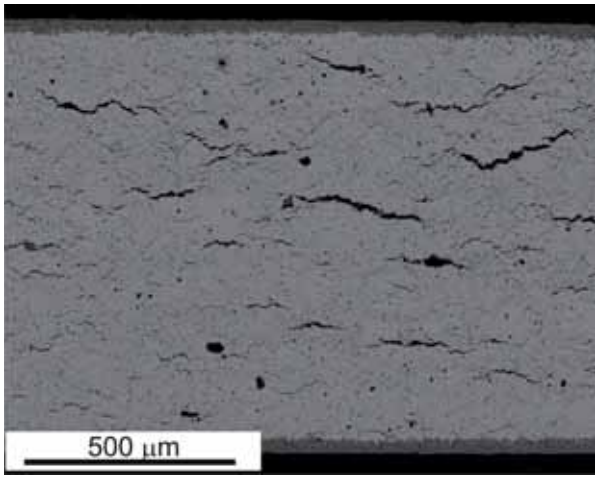

Fig. 4. Cross section of a $CoSb_3$ specimen oxidised at 700°C for 60 h.

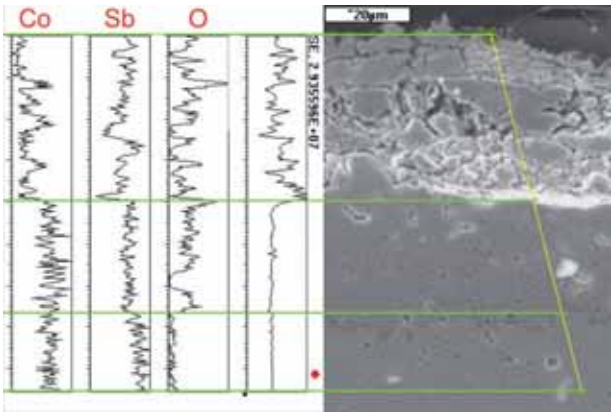

Fig. 5. EDS concentration profiles of elements along the marked line for the uncoated $CoSb_3$ specimen after exposure to air at 600°C/80h.

oxygen concentration measured from the specimen surface and antimony decrease in the opposite direction (Fig. 5). The atomic ratio Co:Sb in the innermost scale layer was about 1:2.

3.2. $CoSb_3$ with a siloxane-Al coating

The surface of specimens with a siloxane-Al coating was examined by SEM before and after the oxidation test. Aluminium lamellae in the coating were oriented parallel to the specimen surface. After the exposure at 500°C, the antimony oxide crystals were small and sparsely distributed on the surface of single-layer and double-layer coatings. After the exposure at 600°C, crystals with different shapes and sizes appeared on the surface of specimens with a single-layer coating (Fig. 6c). Their phase composition was in good agreement with the results of XRD analysis of uncoated specimens oxidised at the same temperature. The composition of dark regions corresponded to the polymer-base coating. Cobalt was not found on the specimen surface. The large crystals composed of antimony oxides on the surface indicated that the single layer polymer-Al coating did not prevent the outward diffusion of antimony. A much better protection was ensured by the double-layer coating, *i.e.* fewer outgrowing crystals were visible on the surface (Fig. 6d).

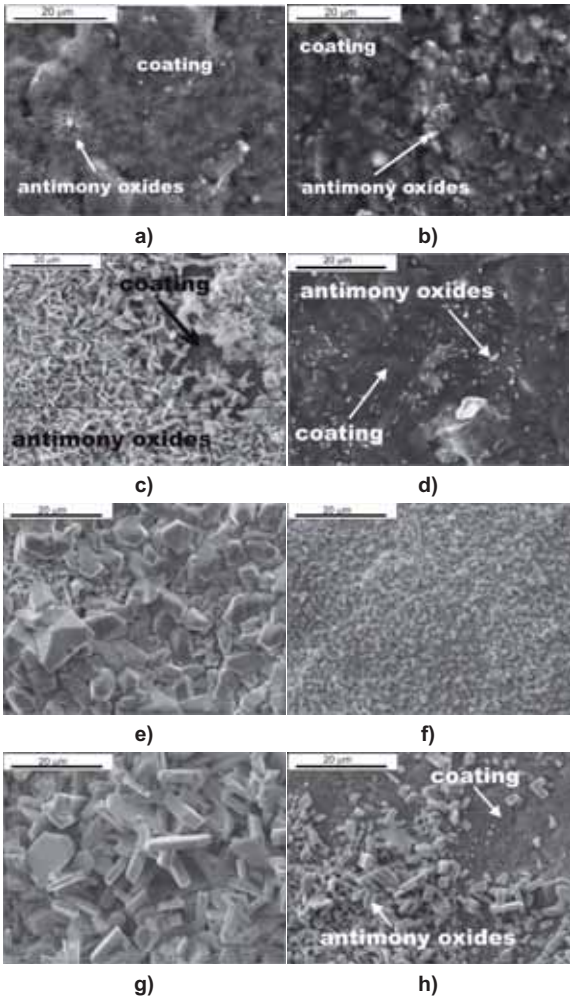

Fig. 6. Surface of $CoSb_3$ samples with polymer-Al coating after exposure a) 500˚C single-layer 80-h b) 500˚C double-layer 80-h c) 600˚C single-layer 80-h d) 600˚C double-layer 80-h e) 700˚C single-layer 40-h f) 700˚C double-layer 40-h g) 700˚C single-layer 80-h h) 700˚C double-layer 80-h.

Moreover, a significant difference could be noticed in the size of crystals, depending on whether the coating was thinner or thicker. On a single-layer coating, the oxide crystals were up to 10 μm in size while on a double-layer coating they are about 2 μm only. On the surface of specimens with a double-layer coating oxidised at 700°C, the oxide crystals were not so diversified in shape and size (Fig. 6h). After 80 h their dimensions attained up to 10 μm. The coating did not perform any better even during the first 40 h of the test (Fig. 6f). Although the crystals were smaller, the surface was thoroughly covered with antimony oxides. Cobalt was not detected on the surface. A much worse result was obtained for the single-layer coating oxidised at 700°C (Figs. 6e and 6g). The oxide crystals on the surface were larger (up to 20 μm) and prone to spallation.

Fig. 7 presents SEM images of fractured specimens with single-layer and double-layer coatings after an 80-h exposure. At 700°C only, oxide crystals appeared on the external surface. Oxide layers under the coating were present on all specimens and their thickness ranged from 5 μm to 20 μm, for the double-layer coating at 500˚C and the single-layer coating at 700°C, respectively. According to EDS analyses those layers were composed of antimony oxides and binary cobalt-antimony oxides. Their thicknesses at 500°C and 600°C were comparable with scale layers on uncoated specimens. Significant differences in scale structure and thickness were noticed after exposure at 700°C. For illustration, thickness of the inner cobalt-antimony oxide layer was 70 μm for the specimen with the double-layer coating and even 200 μm for one with the single-layer coating. Thus, coating thickness had an important impact on the inward transport of oxygen and outward transport of antimony.

3.3. $CoSb_3$ with a siloxane-Cr coating

Similarly as in the case of uncoated specimens, the mass gains of the coated specimens increased with oxidation time and temperature. Table 2 shows the rate of scale growth, expressed as a percent mass change in 20-h intervals. Slight mass losses, recorded for the specimen oxidised at 500°C, might be related to evaporation of some volatile components of the coating. At higher temperatures, this effect was compensated for by faster formation of solid oxides.

For the uncoated specimens the strongest oxygen uptake was recorded during the second cycle and for the specimens with the polymer-Cr coating – during the first cycle. This effect was probably associated with oxidation of chromium in the coating and suppressed vaporisation of antimony oxides.

SEM images of specimen surface after exposure are presented in Fig. 8. Small crystals, visible after oxidation at 500°C and 600°C, were composed of chromium oxide,

Table 2. Average percent mass change of $CoSb_3$ specimens with a polymer-Cr coating during consecutive oxidation cycles.

	Mass changes [%]			
Temp.	0h-20h	20h-40h	40h-60h	60h-80h
500°C	-0.31	0.02	0.02	0.05
600°C	0.29	0.16	0.08	0.26
700°C	2.41	1.98	1.15	0.44

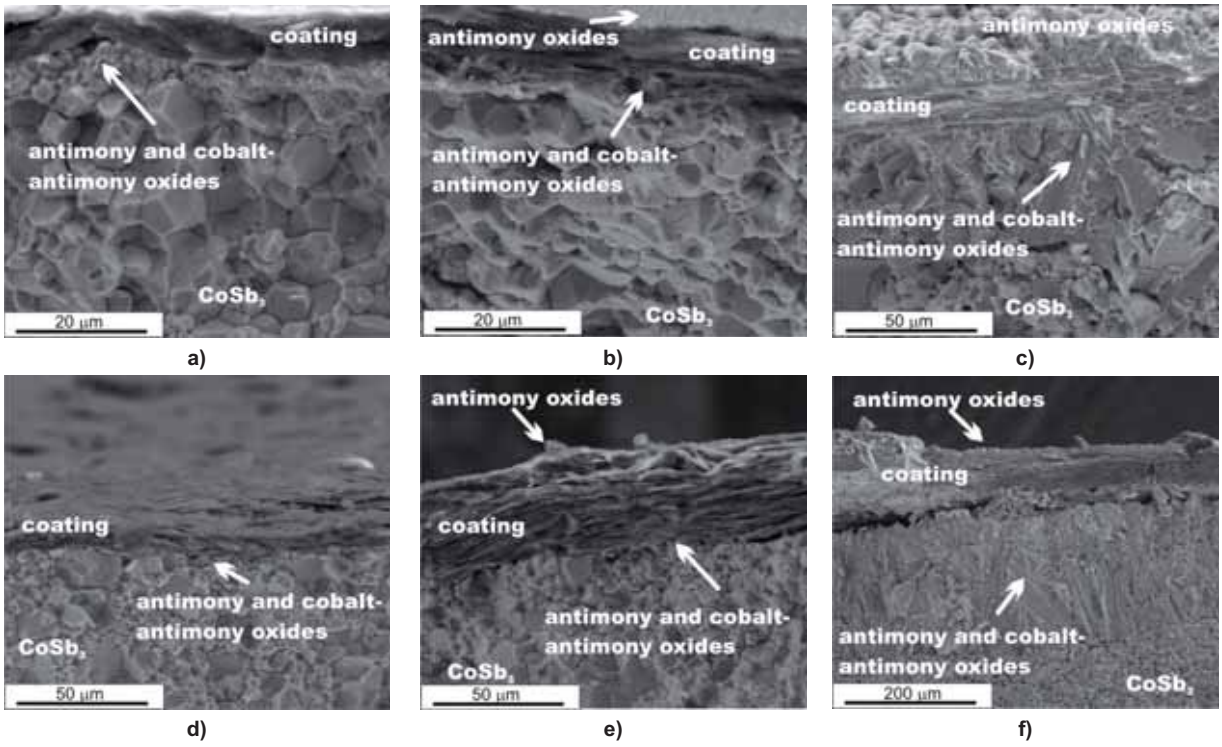

Fig. 7. Fractures of specimens with a single-layer polymer-Al coating oxidized at: a) 500°C, b) 600°C, c) 700°C, and a double-layer coating oxidized at: d) 500°C, e) 600°C, f) 700°C.

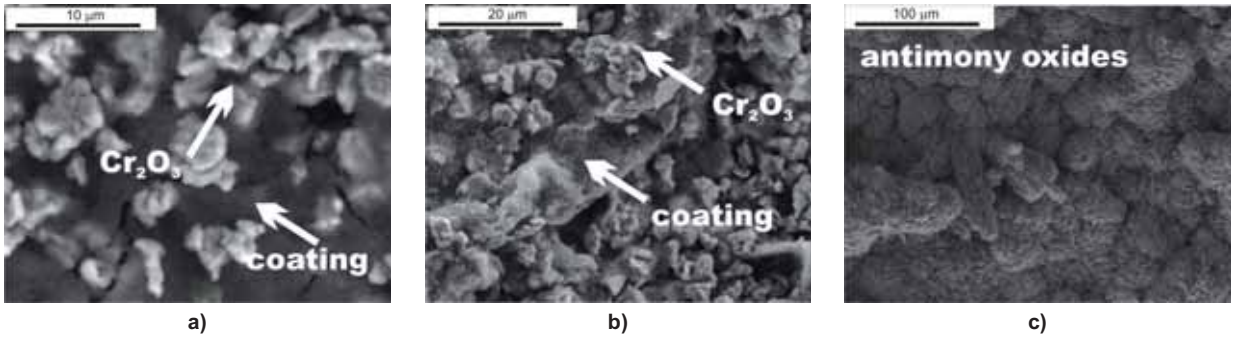

Fig. 8. Surface of $CoSb_3$ with a polymer-Cr coating after an 80-h exposure at: a) 500°C, b) 600°C, c) 700°C.

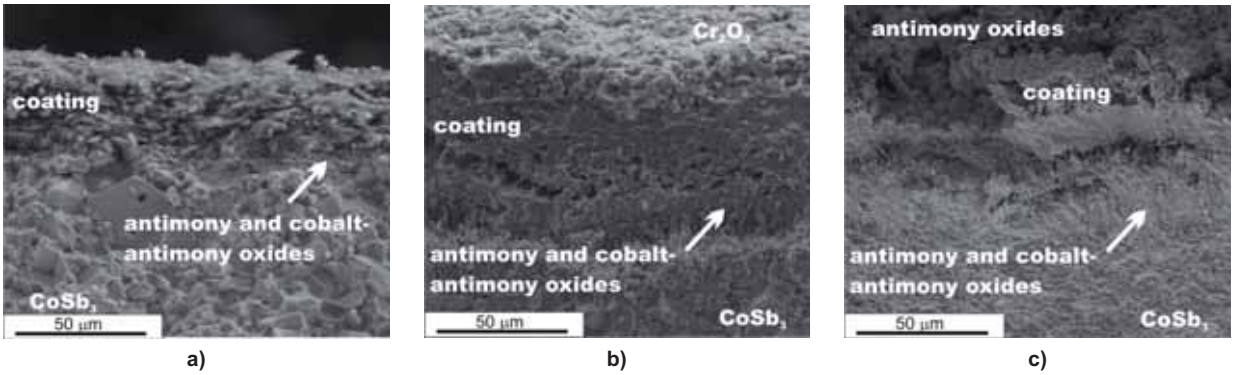

Fig. 9. Fractures of specimens with the polymer-Cr coatings after an 80-h oxidation in air at a) 500°C, b) 600°C, c) 700°C.

Cr_2O_3. Chromium easily reacts with oxygen at these temperatures and its oxide could provide an additional protection. Neither antimony nor cobalt was detected on the surface, which indicates that the polymer-Cr coating was effective in preventing the outward diffusion of those two elements. At 700°C, however, antimony oxide was present again on the coating surface. Cobalt was found in few points only, near the areas where the coating spalled off.

The analyses of specimen fractures and cross-sections after oxidation at 500°C and 600°C demonstrated that some oxide phase formed under the polymer-Cr coating. Thus, while being effective in preventing the loss of antimony, the coating could not eliminate oxygen access to the alloy. In a thin 3-μm oxide layer situated just under the coating on a specimen oxidised at 500°C (Fig. 9a), the EDS spectrum showed Sb, Co and O and the same elements were detected

in a 25 μm layer on the specimen oxidised at 600°C (Fig. 9b). At 700°C, two oxide layers formed under the coating (Fig. 9c). The layer adjacent to the coating was 70 μm thick and the innermost one was up to 200 μm thick. It addition, a wide internal oxidation zone, extending over some 200 μm, appeared in the substrate (Fig. 10).

The oxidation products were identified by XRD. The powdered scale removed from the specimens oxidised at 700°C and the bare specimen surface were analysed separately. The powder contained Sb_2O_4, $CoSb_2O_6$ and β-Sb_2O_4. Phases identified on the specimen surface were $CoSb_3$ and cobalt antimony oxides. The intermediate layer consisted of antimony oxides and cobalt antimony oxides.

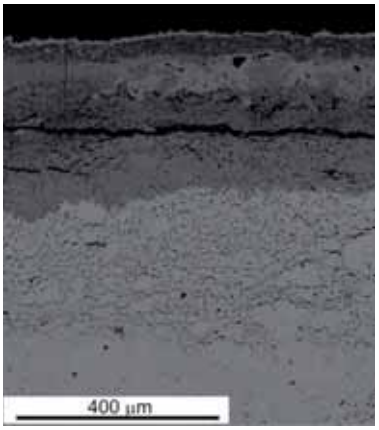

Fig. 10. Cross-section of a $CoSb_3$ with polymer-Cr coating specimen oxidised at 700°C for 80 h.

4. Conclusions

It has been shown that unprotected $CoSb_3$ degrades very fast when exposed to air in the temperature range where its thermoelectric properties are optimal. Antimony reacts rapidly with oxygen and the substrate becomes enriched in cobalt. At 500°C the scale is single-layer and built of antimony oxides. At higher temperatures it becomes double-layer at 600°C or even more complex at 700°C. The inner layers are composed of binary cobalt-antimony oxides. There are clear indications of internal oxidation of $CoSb_3$ beneath the oxide scale.

The oxidation mechanism of $CoSb_3$ involves outward diffusion of antimony and inward diffusion of oxygen.

The extensive internal oxidation takes place along the grain boundaries of the substrate.

The protection provided by the polymer-metal coating depends largely on its composition (type of metallic filler) and the number of layers applied:

– A single-layer coating with the Al filler is not protective. The double-layer coating is only slightly better but it is prone to spallation during the cyclic oxidation test in air;
– The double-layer coating with the Cr filler remarkably limits the loss of antimony up to 600°C but it is not sufficient to stop inward penetration of oxygen.

At 700°C neither of the investigated coatings is capable of reducing the degradation of $CoSb_3$.

Further studies are underway to better understand the properties of Co-Sb-O system and to develop a more effective protection against oxidation of $CoSb_3$ at elevated temperatures.

Acknowledgements

This work was supported by the EEA Financial Mechanism and the Norwegian Financial Mechanism, (Grant no PL0089-SGE-00104-E-V2-EEA, 2007–2010).

References

[1] Fleurial J.P., Borshchevsky A., Caillat T.: „High Figure of Merit in Ce-Filled Skutterudites", Proc. 15th International Conference on Thermoelectrics, Pennington, NJ (1996) 91-95.
[2] Savchuk V., Boulouz A., Chakraborty S., Schumann J., Vinzelberg H.: „Transport and structural properties of binary skutterudite $CoSb_3$ thin films grown by dc magnetron sputtering technique", J. Appl. Phys., 92, (2002), 5319-5326.
[3] Wojciechowski K.T., Leszczynski J., Gajerski R.: „Thermal durability studies of pure and Te-doped $CoSb_3$", Proc. 7th European workshop on Thermoelectrics, Pamplona, Spain (2002).
[4] Hara R., Inoue S., Kaibe H.T, Sano S.: „Aging effects of large-size n-type $CoSb_3$ prepared by spark plasma sintering", J. Alloys Compd, 349, (2003), 297-301.
[5] Leszczynski J., Malecki A., Wojciechowski K.T.: „Comparison of thermal oxidation behavior of $CoSb_3$ and CoP_3, Proc. 5th European Conference on Thermoelectrics, Odessa, Ukraine (2007).
[6] Saber H.H., El-Glenk M.S., Caillat T.: „Test results of skutterudite based thermoelectric unicouples", Energy Conversion and Management, 48, (2007), 555-567.
[7] *Patent No. US7480984 B1, January 2009.*
[8] Dynys F.W, Nathal M.V., Nesbitt J.A., Opila E.J., Sayir A.: *Research & Technology, 2006, NASA* Glenn Research Center, Cleveland, Ohio, (2006), *254.*

♦

Received 1 March 2010; accepted 8 May 2010